Published in final edited form as:
Biomaterials. 2014 August ; 35(26): 7460–7469. doi:10.1016/j.biomaterials.2014.05.055.

Articular chondrocytes and mesenchymal stem cells seeded on biodegradable scaffolds for the repair of cartilage in a rat osteochondral defect model

Rebecca L. Dahlin, **Lucas A. Kinard**, **Johnny Lam**, **Clark J. Needham**, **Steven Lu**, **F. Kurtis Kasper**, and **Antonios G. Mikos***
Department of Bioengineering, Rice University, Houston, Texas USA

Abstract

This work investigated the ability of co-cultures of articular chondrocytes and mesenchymal stem cells (MSCs) to repair articular cartilage in osteochondral defects. Bovine articular chondrocytes and rat MSCs were seeded in isolation or in co-culture onto electrospun poly(ε-caprolactone) (PCL) scaffolds and implanted into an osteochondral defect in the trochlear groove of 12-week old Lewis rats. Additionally, a blank PCL scaffold and untreated defect were investigated. After 12 weeks, the extent of cartilage repair was analyzed through histological analysis, and the extent of bone healing was assessed by quantifying the total volume of mineralized bone in the defect through microcomputed tomography. Histological analysis revealed that the articular chondrocytes and co-cultures led to repair tissue that consisted of more hyaline-like cartilage tissue that was thicker and possessed more intense Safranin O staining. The MSC, blank PCL scaffolds, and empty treatment groups generally led to the formation of fibrocartilage repair tissue. Microcomputed tomography revealed that while there was an equivalent amount of mineralized bone formation in the MSC, blank PCL, and empty treatment groups, the defects treated with chondrocytes or co-cultures had negligible mineralized bone formation. Overall, even with a reduced number of chondrocytes, co-cultures led to an equal level of cartilage repair compared to the chondrocyte samples, thus demonstrating the potential for the use of co-cultures of articular chondrocytes and MSCs for the *in vivo* repair of cartilage defects.

Keywords

Articular chondrocyte; Mesenchymal stem cell; Co-culture; Rat osteochondral defect; Cartilage regeneration

*Corresponding Author: Antonios G. Mikos, Ph.D., Rice University, 6100 Main Street, Department of Bioengineering – MS 142, P.O. Box 1892, Houston, TX 77005, Tel.: +1 713 348 5355, mikos@rice.edu.

Introduction

While a number of treatment options currently exist for the repair of articular cartilage defects, these options primarily lead to short-term functional repair, but are not capable of achieving stable, long-term repair of the tissue [1, 2]. Autologous chondrocyte implantation (ACI) is generally one of the most often-used procedures for the treatment of cartilage defects, and has been shown to have some success in repairing the damaged tissue [1, 3]. However, the isolation of appropriate numbers of autologous chondrocytes is not without challenges. Chondrocytes are present in relatively low densities in native articular cartilage [4], and the isolation of sufficient numbers would lead to large donor site morbidity [5]. Furthermore, the *in vitro* expansion of chondrocytes is associated with a rapid dedifferentiation of the cells into a more fibroblastic phenotype, which ultimately leads to the production inferior tissue [6]. Thus, numerous approaches have been investigated in order to enhance the chondrogenic phenotype of expanded cells or to reduce the demand for chondrocytes in the treatment of articular cartilage defects [7].

Co-cultures of articular chondrocytes and mesenchymal stem cells (MSCs) are one approach that has been proposed to reduce the demand for articular chondrocytes and thus improve articular cartilage treatments [8–11]. When co-cultured with MSCs, articular chondrocytes have been observed to undergo enhanced proliferation and matrix production [9, 12–14]. This effect, which has been shown to be independent of MSC source or culture condition [15], would allow for the use of reduced numbers of chondrocytes to achieve an equal chondrogenic outcome [11]. Furthermore, the co-cultured cell population has been demonstrated to be more sensitive to chondrogenic stimuli, such as transforming growth factor-β3 (TGF-β3), and to produce a phenotype that is more stable after the removal of the stimuli, compared to monocultures of either cell type [8]. While the beneficial effects of MSCs on chondrocytes are crucial to the performance of these co-cultures, chondrocytes have similarly been demonstrated to have beneficial effects on MSCs, which mitigates some disadvantages associated with MSC chondrogenesis. The chondrogenesis of MSCs is challenged by the eventual hypertrophy and mineralization of these cells after extended culture in chondrogenic conditions [16]. However, co-culture with articular chondrocytes has been demonstrated to reduce the hypertrophy of MSCs in culture [10, 17, 18]. Thus, the advantages of co-cultures of articular chondrocytes and MSCs for the *in vitro* generation of articular cartilage is well-documented; however the use of this cell population for *in vivo* repair of articular cartilage defects has not been investigated.

The objective of the present study was to investigate the use of co-cultures of articular chondrocytes and bone marrow-derived MSCs for the *in vivo* repair of articular cartilage in a rat osteochondral defect. We hypothesized that the use of co-cultures of chondrocytes and MSCs would lead to equal or greater cartilage repair compared to chondrocytes alone, thus allowing for the use of reduced numbers of chondrocytes. Therefore, we implanted electrospun poly(ε-caprolactone) (PCL) scaffolds, seeded with MSCs, chondrocytes, or co-cultures of chondrocytes and MSCs into the trochlear groove of rats and evaluated the tissue repair via histology and microcomputed tomography.

Methods

Study design

The groups investigated in this study are outlined in Table 1. Briefly, bovine articular chondrocytes and rat bone marrow-derived MSCs were seeded onto electrospun PCL scaffolds to create three separate experimental groups. The AC group consisted of articular chondrocytes seeded in monoculture at a density of 40,000 cells per scaffold; the MSC group consisted of MSCs seeded in monoculture at a density of 40,000 cells per scaffold. The CC group consisted of articular chondrocytes and MSCs seeded in a 1:3 ratio at a density of 40,000 cells per scaffold (i.e. 10,000 chondrocytes and 30,000 MSCs). Additionally, an empty control (empty) and a material control (PCL) were also investigated. All samples (n=8 per group) were implanted into defects created in the trochlear groove of Lewis rats for 12 weeks. Samples were analyzed for cartilage tissue formation through histological scoring and for the formation of mineralized bone through microcomputed tomography.

Scaffold fabrication

Non-woven mats were electrospun using PCL (Sigma-Aldrich, St. Louis, MO) with a number-average molecular weight (Mn) of 114,000 ± 4,000 Da and a polydispersity index (Mw/Mn) of 2.02 ± 0.04, as determined by gel permeation chromatography (Phenogel Linear Column with 5-μm particles, Phenomenex, Torrance, CA; Differential Refractometer 410, Waters, Milford, MA, n=3) and a calibration curve generated from polystyrene standards (Fluka, Switzerland). Briefly, a 14 wt% solution of PCL was prepared by dissolving the polymer in a 5:1 volume ratio of chloroform to methanol. The polymer solution was extruded at 25 ml/h through a 16 G needle, charged to 30 kV, towards a grounded collecting plate 40 cm away. Fiber morphology was inspected using scanning electron microscopy and determined to be 9.51±0.75 μm (n=32 fibers). Scaffolds were punched from mats using a 1.5 mm dermal biopsy punch. Scaffolds approximately 1.6 mm in thickness were used for this study.

After preparation, scaffolds were loaded into custom-designed polycarbonate blocks designed to confine the cell suspension during seeding and sterilized by exposure to ethylene oxide (Anderson Sterilizers, Haw River, NC) for 14 h. Scaffolds were then prewet by soaking in a graded ethanol series, rinsed in phosphate buffered saline (PBS) three times, and soaked in general medium (DMEM, 10% FBS, 1% PSF) for 72 h.

Cell isolation and culture

Bovine articular chondrocytes were isolated from the femoral chondyles of 7 to 10-day old calves (Research 87, Boylston, MA) within 24 h of slaughter using previously described methods [19]. Briefly, cartilage was isolated, minced to 1×1×1 mm pieces, washed with PBS, and incubated in chondrocyte growth medium (DMEM, 10% FBS, 1% non-essential amino acids, 50 μg/ml ascorbic acid, 46 μg/ml L-proline, 20 mM HEPES, 1% PSF) supplemented with 2 mg/ml collagenase type II (Worthington biochemical corporation, Lakewood, NJ) on a shaker table at 37°C for 16 h. Cells were isolated from 4 legs, pooled,

aliquoted and cryopreserved in freezing medium (DMEM containing 20% FBS and 10% dimethyl sulfoxide).

MSCs were isolated from the femora and tibiae of five 6-week old, male Lewis rats (150–174 g; Harlan Laboratories, Indianapolis, IN) [20]. Care of the animals was provided in accordance with the Rice University Institutional Animal Care and Use Committee. Isolation was performed using previously described methods [20]. Briefly, after euthanasia, the tibiae and femora were aseptically removed and the marrow was flushed from each bone using 5 ml of general media. Marrow pellets were collected, broken up, and plated in 75-cm^2 tissue culture flasks. Medium was replaced after one day in order to remove the non-adherent cell population. Cells were cultured for 5 days, after which they were lifted using 0.05% trypsin-EDTA, pooled, and cryopreserved in freezing medium for storage.

MSCs and chondrocytes were then thawed, plated, and expanded in chondrocyte growth medium for 5 days. Cells were then lifted using 0.05% trypsin-EDTA, suspended in chondrocyte growth medium. 30 μl of cell suspension, containing 40,000 cells, was pipetted on top of each scaffold. Scaffolds were seeded with MSCs, chondrocytes, or a 1:3 mixture chondroctyes and MSCs. Scaffolds were then incubated overnight to allow for cell attachment. Empty scaffolds were also incubated for an additional night after prewetting in chondrocyte growth medium. Prior to implantation scaffolds were removed from loading blocks and rinsed in sterile PBS.

Animal surgeries

Animal surgeries were performed according to protocols approved by the Rice University Institutional Animal Care and Use Committee, and NIH guidelines for the care and use of laboratory animals (NIH Publication #85–23 Rev. 1985) were observed. Forty healthy male Lewis rats (12-weeks old and weighing 300–350 g) were purchased from Harlan Labs (Indianapolis, IN). Animals were anesthetized in an induction chamber with a 4% isofluorane/oxygen gas mixture. Prior to surgery, each animal was given an intraperitoneal injection of buprenorphine, an intraperitoneal injection of normal saline to account for fluid losses during surgery, a subcutaneous injection of enrofloxacin as a prophylaxis against infection during surgery, and a subcutaneous injection of bupivacaine along the intended line of incision. Additionally, post-operatively each animal was given periodic intraperitoneal injections of buprenorphine for post-operative analgesia.

During surgery, a lateral parapatellar longitudinal incision was made to expose the knee joint. The synovial capsule was incised, and the trochlear groove was exposed after medial luxation of the patella. With the knee maximally flexed, a defect (1.5 mm in diameter, and 1.5 mm in depth) was created in the center of the groove, using a dental drill. A 0.9 mm diameter drill bit was first used to establish a 0.9 mm diameter defect. The defect was irrigated and enlarged to 1.5 mm using a 1.5 mm drill bit, fashioned with a 1.5 mm stop to ensure a defect of precisely 1.5 mm in depth is created. All debris was removed from the defect with a curette and irrigation. Depending on the experimental group, the defect was left untreated or a scaffold was press-fit into the defect with the appropriate cell population. The patella was physically relocated, and the joint capsule and subcutaneous tissue was closed with Vicryl 5–0 sutures. The skin was closed with Vicryl 4–0 sutures, which were

removed after 1 week. After 12 weeks animals were euthanized via CO_2 asphyxiation and tissue surrounding the trochlear groove was removed en bloc. Samples were fixed in 10% neutral buffered formalin for 72 h at room temperature. Following fixation samples were stored in 70% ethanol.

μCT imaging and analysis

After tissue fixation the volume of mineralized bone in the defect was analyzed by microcomputed tomography (Skyscan 1172 high-resolution micro-CT; Sky-scan) using previously established methods [21]. To determine the volume of bone in the defect, a region of interest 1.5 mm in diameter and 1.5 mm in thickness was selected by defining the bottom region of the defect and measuring 1.5 mm toward the joint surface. The total volume of mineralized bone was then calculated using thresholds 45 and 255.

Tissue processing

Samples were demineralized with EDTA and formic acid (Formical 2000; Decal Corporation, Congers, NY) for 3 weeks on a shaker table at room temperature. Samples were then prepared for crysosectioning by soaking in a solution of PBS with 15 wt% sucrose, followed by PBS with 30% sucrose. Samples were then frozen in Histoprep freezing medium at a controlled rate using chilled 2-methylbutane, and sectioned using a cryotome (Leica CM 1850 UV; Leica Biosystems Nussloch GmbH, Germany). Longitudinal sections 6 μm thick were mounted on glass slides. Sections were stained with Safranin O/Fast Green and hematoxylin and eosin (H&E). Images were obtained using a light microscope with a digital camera attachment (Axio Imager.Z2 equipped with AxioCam MRc5; Carl Zeiss MicroImaging GmbH, Germany).

Histological scoring

Histological sections from the lateral and medial regions of each defect (total of 16 images per group) were blindly scored by three independent evaluators (J.L., S.L., L.A.K.) based on a modified version of a previously established scoring system for osteochondral tissue repair in rabbits [22]. Sections were scored for the extent of cartilage repair based on 8 criteria, as shown in Table 2.

Statistical analysis

A significance level of 0.05 was used for all statistical analysis. μCT data was analyzed by one-way analysis of variance and Tukey's multiple-comparision test. Data are reported as means plus the standard deviation. Histological scores were analyzed using the Kruskal-Wallis test followed by the Mann-Whitney-U test. Data are reported as the distribution of scores for each parameter.

Results

μCT imaging and analysis

μCT analysis (Figure 1) found mineralized bone regeneration in the empty, blank, and MSC samples that resulted in 28–35% of the defect site filled with new bone. No effect of the

PCL scaffold or MSCs was observed on the total mineralized bone volume in the defect. In the AC and CC samples, negligible mineralized bone growth was observed with a total bone volume of only 0.75–1.0% of the defect site. Thus, significantly lower mineralized bone volume was detected in the AC and CC samples compared to the empty, blank or MSC samples.

Histological observation and scoring

Representative images of the histological sections from each group are shown in Figures 2–6, while Figures 7 and 8 show the score distributions for each of the 8 parameters listed in Table 2.

In general, the surface tissue of the empty samples contained large amounts of fibrous tissue or fibrocartilage with only one sample containing any hyaline cartilage on the surface. The vast majority of PCL and MSC samples only had a thin layer of fibrous tissue on the surface of the defect. CC and AC samples often had hyaline-like cartilage on the edges or interior of the defect with a portion of fibrous tissue in the center of the defect surface. In scoring the morphology of new surface tissue, it was observed that the CC samples had higher quality surface tissue compared to PCL and MSC samples.

When evaluating the morphology of the new cartilage tissue that formed in the defect site (Fig. 7C) it was again seen that nearly all the empty, PCL, and MSC samples resulted in either no cartilage growth in the defect site or cartilage that consisted almost exclusively of fibrocartilage. However, a large portion of the CC and AC samples contained primarily hyaline cartilage, rather then fibrocartilage, and while some had either no cartilage tissue or primarily fibrocartilage, histological scoring still resulted in significantly higher quality cartilage in the CC and AC samples then in the empty, PCL, and MSC samples.

Consistent with the evaluation of cartilage morphology, the evaluation of Safranin O staining in the defects revealed more intense staining in the CC and AC samples compared to the empty, PCL, and MSC groups. Little to no Safranin O staining was observed in the PCL and MSC samples, and similarly 15 of 16 images analyzed from the empty samples contained little to no Safranin O staining.

When evaluating the thickness of new cartilage tissue, fibrocartilage in the empty, PCL, and MSC groups was generally found to be thinner than the neighboring cartilage thickness. In the CC and AC samples, the new cartilage tissue was generally found to be thicker than the neighboring tissue. Histological scoring found that CC and AC samples had significantly thicker cartilage tissue then the empty PCL, and MSC samples.

When evaluating the density of chondrocytes in the new cartilage tissue, it was observed that the AC samples scored significantly higher than the empty, PCL, and MSC samples, and the CC samples had higher scores then the PCL samples. While a higher score would indicate a more desirable outcome, and ideally a chondrocyte density most similar to the neighboring cartilage, it should be noted that both the CC and AC groups had a large portion of samples with a higher density of chondrocytes compared to the surrounding tissue.

Evaluating the distribution of chondrocytes in the tissue, it was observed that the empty, PCL, and MSC samples mostly consisted of individual or disorganized cells, whereas CC and AC samples primarily consisted of clustered chondrocytes. Thus, the CC and AC groups scored significantly higher in chondrocyte distribution compared to the empty, PCL, and MSC samples.

When evaluating the regularity of the joint surface as well as the chondrocyte and GAG content of the adjacent cartilage, it was observed that the AC samples had significantly worse joint regularity than the empty, PCL, or MSC samples and the CC samples had worse regularity than the PCL samples. However, the CC samples were seen to have higher quality adjacent cartilage than the empty, PCL, and MSC samples.

Consistent with the results of μCT analysis, significant bone ingrowth was observed throughout the empty, PCL, and MSC samples (Fig. 2–4). Conversely, negligible bone growth was observed in the CC and AC samples. Instead, the scaffold was primarily surrounded by fibrous tissue (Fig. 5E and 6E) with transitional tissue (Fig. 5D and 6D)[23] observed in the interior of the scaffold. The ingrown tissue had no Safranin O staining, and contained cells that were either oval or spheroid in shape with some present in lacunae (Fig. 6D).

Discussion

Clinically, autologous chondrocytes have long been recognized for their ability to repair chondral defects when transplanted *in vivo* [3]. Currently, the ACI procedure involves initial biopsy of autologous cartilage for the isolation of articular chondrocytes, expansion of cells *in vitro*, and implantation of expanded cells into the defect, which is sealed by a layer of periosteum sutured over top [1]. While the technique is widely used in the clinic, the use of autologous chondrocytes presents several challenges to the long-term success of the treatment. Isolating large numbers of chondrocytes from healthy cartilage not only leads to donor site morbidity, but also is a challenge due to the relatively low density of chondrocytes in cartilage tissue [4]. Furthermore, rapid phenotypic changes are seen during *in vitro* expansion of chondrocytes, which leads to a cell population with a more fibroblastic phenotype than healthy articular chondrocytes [6]. Co-cultures of articular chondrocytes and MSCs have previously been shown, through *in vitro* analysis, to be able to provide several potential means to overcome some of the challenges posed by the use of articular chondrocytes alone [8, 9, 11].

Co-culture of articular chondrocytes and MSCs have been thoroughly investigated *in vitro*, and the utility of this approach has generally been shown to be the ability to use up to 75% fewer chondrocytes, while still achieving equal or greater levels of chondrogenesis as cultures containing 100% chondrocytes [9, 11]. While numerous studies have characterized these cultures in *vitro*, they have not been investigated for their ability to regenerate cartilage in an orthotopic site *in vivo*. The objective of the present study was to evaluate the ability of co-cultures of chondrocytes and MSCs to repair articular cartilage in a rat osteochondral defect when implanted with an electrospun polymer scaffold. We hypothesized that such co-cultures would lead to equal or greater cartilage repair, while utilizing significantly fewer

chondrocytes, than chondrocytes alone. For consistency with previous *in vitro* studies [8–11], we chose to use a 1:3 ratio of chondrocytes-to-MSCs seeded on electrospun PCL scaffolds. The animal model chosen for this study was a previously established osteochondral defect in the rat trochlear groove [24, 25]. Due to the impracticality of isolating rat cartilage, bovine articular chondrocytes were used for this study. Even using xenogeneic chondrocytes in this model, we observed no evidence of an immune response to the bovine cells in either the AC or CC groups. In addition we observed hyaline-like cartilage formation in these samples, demonstrating that the implanted cells were beneficial to the tissue repair. Several other studies have demonstrated similar success with xenogenic chondrocytes in chondral and osteochondral defects without signs of an immune response [26, 27].

As hypothesized, chondrocytes and co-cultures of chondrocytes and MSCs led to enhanced cartilage repair *in vivo*, as primarily characterized by repair tissue that consisted of thicker hyaline-like cartilage with more intense Safranin O staining. Conversely, new cartilage formed in the empty, PCL, and MSC samples primarily consisted of fibrocartilage, a common form of repair tissue composed primarily of collagen type I and low amounts of type II collagen and proteoglycans [28]. Due to the inferior mechanical properties of this tissue composition, compared to hyaline cartilage, the fibrocartilage is not expected to withstand long-term mechanical loading and may deteriorate over time [2]. Consistent with this tissue characterization, the CC and AC samples were found to have more intense Safranin O staining than the other samples, indicative of higher proteoglycan content and a more hyaline-like tissue [29]. Furthermore, new cartilage formed in the CC and AC samples was not only of a superior morphology but was found to be much thicker than new cartilage formed in the empty, PCL, and MSC samples. This result is correlated to the ability of the different treatments to form cartilage but may also be due to deterioration of repair cartilage prior to twelve weeks in the empty, PCL, and MSC samples. Based on the histological scoring, the adjacent cartilage of the empty, PCL, and MSC samples showed signs of degenerative changes, relative to the CC samples, providing evidence of the likelihood of past or future deterioration of the repair tissue. Investigation of additional time points in future studies would likely shed light on the long-term stability of this tissue. Additionally, the distribution of cells in the CC and AC samples was found to be more similar to native cartilage, again indicating an improved healing response compared to empty, PCL, and MSC samples. Overall, it was observed that the CC and AC samples led to the formation of new cartilage tissue with a higher quality composition and structure compared to the empty, PCL, and MSC samples. The quality of this tissue is more similar to native hyaline cartilage and would be expected to be a more functional and durable tissue compared to the fibrocartilage seen in the other samples.

While the newly formed cartilage of the CC and AC samples was in many ways significantly higher quality repair tissue than the empty, PCL, and MSC samples, the surface regularity of the AC samples was worse than all groups other than CC. This may be a result of the large amount of cartilage formation that did not integrate well with the surrounding tissue: a significant challenge in cartilage repair [2]. Alternatively, the poor surface regularity could be a result of the lack of bone formation in the subchondral region, and thus

lack of stability of the newly formed tissue [30, 31]. Furthermore, in many instances, the new cartilage tissue in the CC and AC samples had a slight concave structure with the center filled with fibrous tissue. This indentation may be further evidence of a lack of underlying structural support in these samples. The drastic difference in bone and cartilage healing that was observed in these samples is quite remarkable when the impact of the subchondral bone in cartilage regeneration is considered. It is well established that the healing of the subchondral bone is crucial to both the regeneration and stability of articular cartilage [32–34], so the stark improvement in cartilage repair seen in samples with no subchondral bone healing at 12 weeks was a significant outcome that demonstrates the robust ability of the CC and AC treatments to stimulate cartilage repair.

Transitional tissue has been described as a tissue that is comprised of ovoid and spherical cells, present with or without lacunae. This tissue characterization encompasses tissues that range from fibrous tissue to hyaline cartilage and includes, but is not limited to, fibrocartilage [23, 35]. Most transitional tissue is of a higher regenerative quality than fibrous tissue, but a lower quality than fibrocartilage [36]. Studies evaluating the quality of new tissue seen in repair procedures have often observed the formation of transitional tissue after the deterioration of hyaline tissue or the presence of transitional tissue without earlier evidence of hyaline cartilage [37–39]. In the present study, transitional tissue was observed to be the primary tissue type that grew into the subchondral region of the CC and AC samples. Without earlier time points, we are unable to determine the initial morphology of the ingrown tissue; however it is possible that this tissue was of a higher quality cartilage repair tissue that deteriorated to its present state. Likewise, it is possible that this tissue would eventually remodel and bone ingrowth would occur into the subchondral regions of the scaffold. However, future studies should investigate the use of a bilayered treatment method that could accelerate the bone healing in the subchondral region of the CC and AC samples. The presence of subchondral support may further enhance the cartilage repair [32, 33].

Interestingly, when seeded on PCL scaffolds, MSCs had no measurable effect on either cartilage healing or mineralized bone volume compared to PCL scaffolds alone. While numerous studies have demonstrated enhanced cartilage [40, 41] repair with the delivery of MSCs, other work has observed no effect of delivered MSCs on cartilage repair [31]. Potentially, the method of cell delivery in this study may have not allowed for condensation of the MSCs. Other studies delivering MSCs in osteochondral defects have been capable of achieving MSC condensation, which is known to enhance chondrogenesis [40]. Furthermore, the delivery of undifferentiated MSCs may not have provided the cells with enough chondrogenic stimuli to lead to cartilage formation. Possibly the use of chondrogenically pre-differentiated MSCs may have seen improved chondrogenesis [42].

The results of the present study indicate the potential for the use of co-cultures of articular chondrocytes and MSCs to be used for *in vivo* repair of articular cartilage defects. The number of cells seeded onto the PCL scaffolds in this study was a density of cells that is approximately three times lower then the density reported for use in clinical ACI procedures [3]. However, the use of a polymer scaffold makes the current approach more similar to matrix-associated ACI procedures, which have been demonstrated to be capable of success

with approximately half the number of cells needed for first generation ACI procedures [43]. Furthermore, these results may indicate the mechanism for success of experimental procedures investigating the combination of ACI with microfracture [23]. Therein it was observed that the combination of ACI with microfracture led to improved cartilage repair compared to ACI alone. Based on the results of the present study, one may postulate that the combination of bone marrow progenitor cells with ACI led to enhanced repair in a similar manner as demonstrated for the effect of co-cultures of MSCs and chondrocytes. Regardless, the results here demonstrate that co-implantation of MSCs with chondrocytes can reduce the total number of chondrocytes needed for implantation when implanted with a total density of cells in the same range as ACI or matrix-associated ACI procedures. The outcome of matrix associated ACI procedures was shown to be dependent on *in vitro* culture conditions, such as the cell passage number [14], and thus the addition of MSCs to chondrocytes may allow for the use of lower passaged chondrocytes and thus improved outcomes.

Conclusions

This study demonstrated the ability of co-cultures of articular chondrocytes and MSCs to repair cartilage defects in the rat trochlear groove defect. These results have important implications for cartilage tissue engineering, as they demonstrate that such co-cultures could be used to reduce the total number of chondrocytes needed for cartilage repair, while still achieving an equivalent level of cartilage repair.

Acknowledgments

This work was supported by the National Institutes of Health grant R01 AR057083.

References

1. Falah M, Nierenberg G, Soudry M, Hayden M, Volpin G. Treatment of articular cartilage lesions of the knee. Int Orthop. 2010; 34:621–30. [PubMed: 20162416]
2. Hunziker EB. Articular cartilage repair: basic science and clinical progress. A review of the current status and prospects. Osteoarthr Cartilage. 2002; 10:432–63.
3. Brittberg M, Lindahl A, Nilsson A, Ohlsson C, Isaksson O, Peterson L. Treatment of deep cartilage defects in the knee with autologous chondrocyte transplantation. New Engl J Med. 1994; 331:889–95. [PubMed: 8078550]
4. Cohen NP, Foster RJ, Mow VC. Composition and dynamics of articular cartilage: structure, function, and maintaining healthy state. J Orthop Sports Phys. 1998; 28:203–15.
5. Matricali GA, Dereymaeker GPE, Luyten FP. Donor site morbidity after articular cartilage repair procedures : a review. Acta Orthop Belg. 2010; 76:669–74. [PubMed: 21138224]
6. Darling EM, Athanasiou KA. Rapid phenotypic changes in passaged articular chondrocyte subpopulations. J Orthop Res. 2005; 23:425–32. [PubMed: 15734258]
7. Hubka KM, Dahlin RL, Meretoja VV, Kasper FK, Mikos AG. Enhancing chondrogenic phenotype for cartilage tissue engineering: monoculture and co-culture of articular Chondrocytes and mesenchymal stem cells for cartilage regeneration. Tissue Eng Part B. 2014 in press. 10.1089/ten.TEB.2014.0034
8. Dahlin RL, Ni M, Meretoja VV, Kasper FK, Mikos AG. TGF-beta3-induced chondrogenesis in co-cultures of chondrocytes and mesenchymal stem cells on biodegradable scaffolds. Biomaterials. 2014; 35:123–32. [PubMed: 24125773]

9. Meretoja VV, Dahlin RL, Kasper FK, Mikos AG. Enhanced chondrogenesis in co-cultures with articular chondrocytes and mesenchymal stem cells. Biomaterials. 2012; 33:6362–9. [PubMed: 22695067]
10. Meretoja VV, Dahlin RL, Wright S, Kasper FK, Mikos AG. The effect of hypoxia on the chondrogenic differentiation of co-cultured articular chondrocytes and mesenchymal stem cells in scaffolds. Biomaterials. 2013; 34:4266–73. [PubMed: 23489925]
11. Meretoja VV, Dahlin RL, Wright S, Kasper FK, Mikos AG. Articular chondrocyte redifferentiation in 3d co-cultures with mesenchymal stem cells. Tissue Eng Part C. 201410.1089/ten.tec.2013.0532
12. Wu L, Leijten JCH, Georgi N, Post JN, van Blitterswijk CA, Karperien M. Trophic effects of mesenchymal stem cells increase chondrocyte proliferation and matrix formation. Tissue Eng Part A. 2011; 17:1425–36. [PubMed: 21247341]
13. Tsuchiya K, Chen GP, Ushida T, Matsuno T, Tateishi T. The effect of coculture of chondrocytes with mesenchymal stem cells on their cartilaginous phenotype in vitro. Mat Sci Eng C-Bio S. 2004; 24:391–6.
14. Mo XT, Guo SC, Xie HQ, Deng L, Zhi W, Xiang Z, et al. Variations in the ratios of co-cultured mesenchymal stem cells and chondrocytes regulate the expression of cartilaginous and osseous phenotype in alginate constructs. Bone. 2009; 45:42–51. [PubMed: 18708174]
15. Wu L, Prins HJ, Helder MN, van Blitterswijk CA, Karperien M. Trophic effects of mesenchymal stem cells in chondrocyte co-cultures are independent of culture conditions and cell sources. Tissue Eng Part A. 2012; 18:1542–51. [PubMed: 22429306]
16. Dickhut A, Pelttari K, Janicki P, Wagner W, Eckstein V, Egermann M, et al. Calcification or dedifferentiation: requirement to lock mesenchymal stem cells in a desired differentiation stage. J Cell Physiol. 2009; 219:219–26. [PubMed: 19107842]
17. Bian L, Zhai DY, Mauck RL, Burdick JA. Coculture of human mesenchymal stem cells and articular chondrocytes reduces hypertrophy and enhances functional properties of engineered cartilage. Tissue Eng Part A. 2011; 17:1137–45. [PubMed: 21142648]
18. Fischer J, Dickhut A, Rickert M, Richter W. Human articular chondrocytes secrete parathyroid hormone-related protein and inhibit hypertrophy of mesenchymal stem cells in coculture during chondrogenesis. Arthritis Rheum. 2010; 62:2696–706. [PubMed: 20496422]
19. Dahlin RL, Meretoja VV, Ni M, Kasper FK, Mikos AG. Hypoxia and flow perfusion modulate proliferation and gene expression of articular chondrocytes on porous scaffolds. AIChE J. 2012; 59:3158–66.
20. Thibault RA, Scott Baggett L, Mikos AG, Kasper FK. Osteogenic differentiation of mesenchymal stem cells on pregenerated extracellular matrix scaffolds in the absence of osteogenic cell culture supplements. Tissue Eng Part A. 2010; 16:431–40. [PubMed: 19863274]
21. Kinard LA, Dahlin RL, Henslee AM, Spicer PP, Chu CY, Tabata Y, et al. Tissue response to composite hydrogels for vertical bone augmentation in the rat. J Biomed Mater Res Part A. 201310.1002/jbm.a.34878
22. Holland TA, Bodde EW, Cuijpers VM, Baggett LS, Tabata Y, Mikos AG, et al. Degradable hydrogel scaffolds for in vivo delivery of single and dual growth factors in cartilage repair. Osteoarthr Cartilage. 2007; 15:187–97.
23. Dorotka R, Windberger U, Macfelda K, Bindreiter U, Toma C, Nehrer S. Repair of articular cartilage defects treated by microfracture and a three-dimensional collagen matrix. Biomaterials. 2005; 26:3617–29. [PubMed: 15621252]
24. Pagnotto MR, Wang Z, Karpie JC, Ferretti M, Xiao X, Chu CR. Adeno-associated viral gene transfer of transforming growth factor-beta 1 to human mesenchymal stem cells improves cartilage repair. Gene Ther. 2007; 14:804–13. [PubMed: 17344902]
25. Coburn JM, Gibson M, Monagle S, Patterson Z, Elisseeff JH. Bioinspired nanofibers support chondrogenesis for articular cartilage repair. Proc Natl Acad Sci USA. 2012; 109:10012–7. [PubMed: 22665791]
26. van Susante JL, Buma P, Schuman L, Homminga GN, van den Berg WB, Veth RP. Resurfacing potential of heterologous chondrocytes suspended in fibrin glue in large full-thickness defects of

femoral articular cartilage: an experimental study in the goat. Biomaterials. 1999; 20:1167–75. [PubMed: 10395385]

27. Ramallal M, Maneiro E, Lopez E, Fuentes-Boquete I, Lopez-Armada MJ, Fernandez-Sueiro JL, et al. Xeno-implantation of pig chondrocytes into rabbit to treat localized articular cartilage defects: an animal model. Wound Repair Regen. 2004; 12:337–45. [PubMed: 15225212]
28. Furukawa T, Eyre DR, Koide S, Glimcher MJ. Biochemical-studies on repair cartilage resurfacing experimental defects in the rabbit knee. J Bone Joint Surg Am. 1980; 62:79–89. [PubMed: 7351420]
29. LR. Chemical basis for histological use of safranin-o in study of articular cartilage. J Bone Joint Surg Am. 1971; 53:69–82. [PubMed: 4250366]
30. Shao XX, Hutmacher DW, Ho ST, Goh JCH, Lee EH. Evaluation of a hybrid scaffold/cell construct in repair of high-load-bearing osteochondral defects in rabbits. Biomaterials. 2006; 27:1071–80. [PubMed: 16129483]
31. Guo X, Park H, Young S, Kretlow JD, van den Beucken JJ, Baggett LS, et al. Repair of osteochondral defects with biodegradable hydrogel composites encapsulating marrow mesenchymal stem cells in a rabbit model. Acta Biomater. 2010; 6:39–47. [PubMed: 19660580]
32. Orth P, Cucchiarini M, Kohn D, Madry H. Alterations of the subchondral bone in osteochondral repair--translational data and clinical evidence. Eur Cell Mater. 2013; 25:299–316. [PubMed: 23813020]
33. Chen H, Chevrier A, Hoemann CD, Sun J, Ouyang W, Buschmann MD. Characterization of subchondral bone repair for marrow-stimulated chondral defects and its relationship to articular cartilage resurfacing. Am J Sports Med. 2011; 39:1731–40. [PubMed: 21628638]
34. Mohan N, Dormer NH, Caldwell KL, Key VH, Berkland CJ, Detamore MS. Continuous gradients of material composition and growth factors for effective regeneration of the osteochondral interface. Tissue Eng Part A. 2011; 17:2845–55. [PubMed: 21815822]
35. Nehrer S, Breinan HA, Ramappa A, Hsu HP, Minas T, Shortkroff S, et al. Chondrocyte-seeded collagen matrices implanted in a chondral defect in a canine model. Biomaterials. 1998; 19:2313–28. [PubMed: 9884045]
36. McGinty, JB.; Burkhart, SS. Operative Arthroscopy. 3. Philadelphia: Lippincott Williams & Wilkins; 2003.
37. Dorotka R, Bindreiter U, Macfelda K, Windberger U, Nehrer S. Marrow stimulation and chondrocyte transplantation using a collagen matrix for cartilage repair. Osteoarthr Cartilage. 2005; 13:655–64.
38. LaPrade RF, Bursch LS, Son EJ, Havlas V, Carlson CS. Histologic and immunohistochemical characteristics of failed articular cartilage resurfacing procedures for osteochondritis of the knee. Am J Sports Med. 2008; 36:360–8. [PubMed: 18006675]
39. Nehrer S, Spector M, Minas T. Histologic analysis of tissue after failed cartilage repair procedures. Clin Orthop Relat Res. 1999:149–62. [PubMed: 10627699]
40. Lim CT, Ren XF, Afizah MH, Tarigan-Panjaitan S, Yang Z, Wu YN, et al. Repair of osteochondral defects with rehydrated freeze-dried oligo[poly(ethylene glycol) fumarate] hydrogels seeded with bone marrow mesenchymal stem cells in a porcine model. Tissue Eng Part A. 2013; 19:1852–61. [PubMed: 23517496]
41. Jung M, Kaszap B, Redohl A, Steck E, Breusch S, Richter W, et al. Enhanced early tissue regeneration after matrix-assisted autologous mesenchymal stem cell transplantation in full thickness chondral defects in a minipig model. Cell Transplant. 2009; 18:923–32. [PubMed: 19523325]
42. Lam J, Lu S, Meretoja VV, Tabata Y, Mikos AG, Kasper FK. Generation of osteochondral tissue constructs with chondrogenically and osteogenically pre-differentiated mesenchymal stem cells encapsulated in bilayered hydrogels. Acta Biomater. 2014; 10:1112–23. [PubMed: 24300948]
43. Zeifang F, Oberle D, Nierhoff C, Richter W, Moradi B, Schmitt H. Autologous chondrocyte implantation using the original periosteum-cover technique versus matrix-associated autologous chondrocyte implantation a randomized clinical trial. Am J Sports Med. 2010; 38:924–33. [PubMed: 19966102]

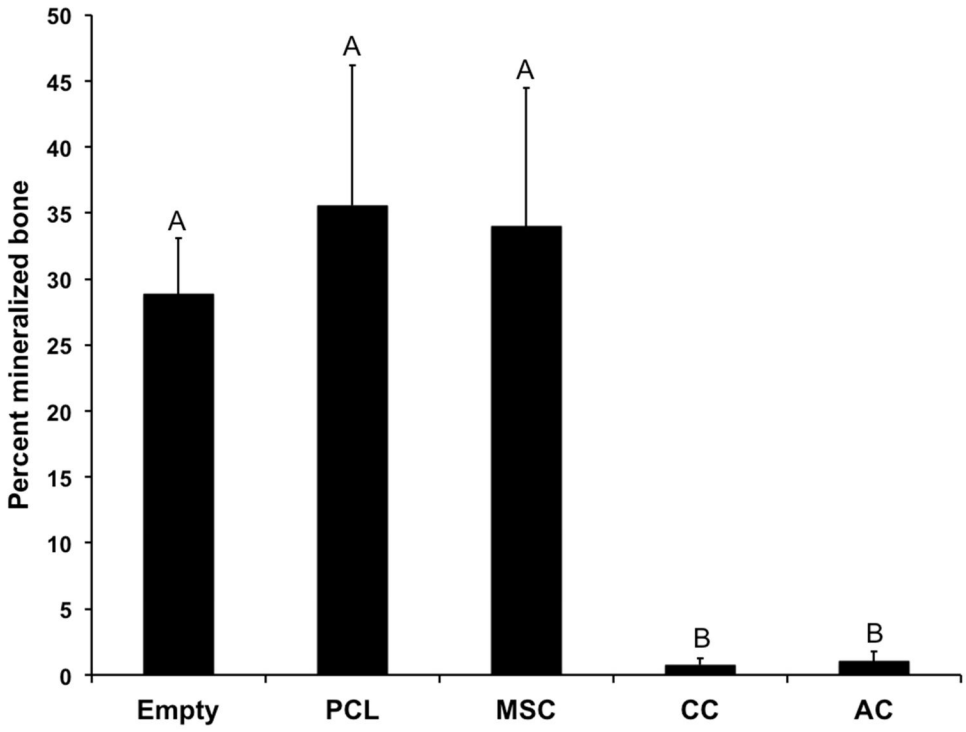

Figure 1.

Percent of defect volume filled with mineralized bone, as determined by microcomputed tomography. Data are reported as means + standard deviation for n=8 animals. Groups not connected by the same letter are significantly different ($p<0.05$).

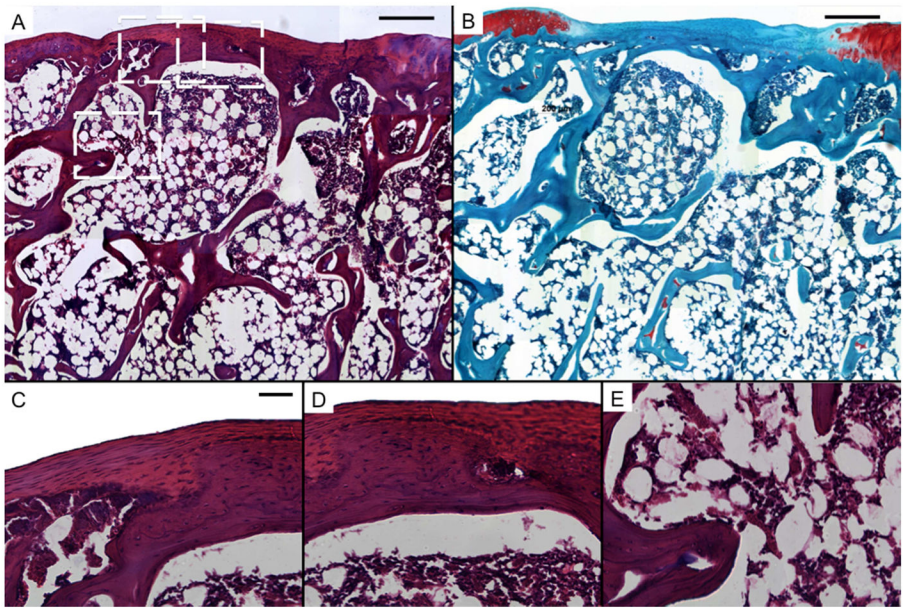

Figure 2.

Representative histological sections of tissue formation after 12 weeks in untreated defects in the rat trochlear groove (empty). Sections were stained with H&E (A, C, D, and E) and Safranin O/Fast Green (B). Scale bars in A and B each represent 250 μm, and scale bar in C represents 50 μm in C, D, and E. A and B show mostly fibrous tissue with limited fibrocartilage in the chondral region and bone growth in the subchondral space. C, D, and E show high magnification images of the chondral and subchondral regions.

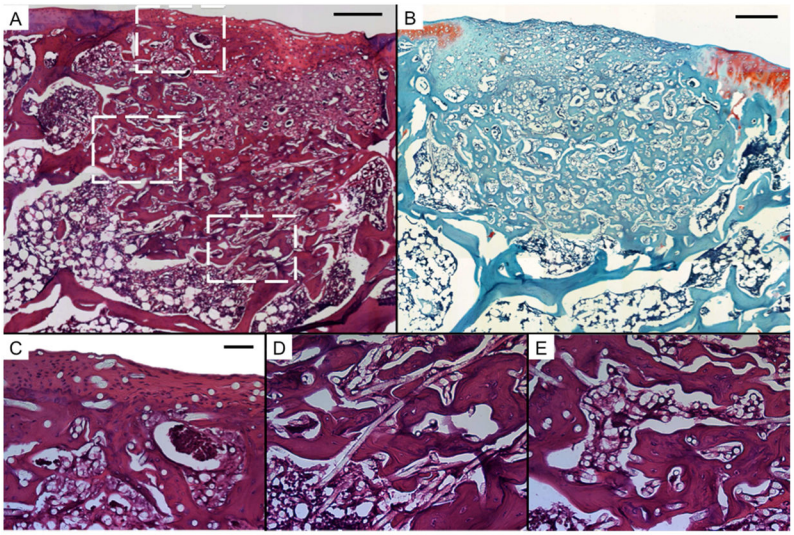

Figure 3.

Representative histological sections of tissue formation after 12 weeks of implantation of electrospun PCL scaffolds (PCL). Sections were stained with H&E (A, C, D, and E) and Safranin O/Fast Green (B). Scale bars in A and B each represent 250 μm, and scale bar in C represents 50 μm in C, D, and E. A and B show mostly fibrous tissue with limited fibrocartilage in the chondral region and new bone growth into the nondegraded PCL scaffold. Round, unstained regions of approximately 10 μm show fibers comprising the PCL scaffold. C, D, and E show high magnification images of the chondral and subchondral regions.

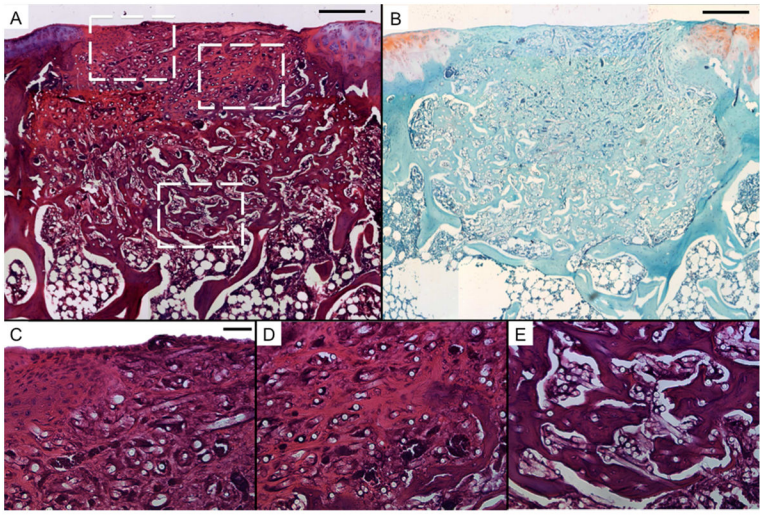

Figure 4.

Representative histological sections of tissue formation after 12 weeks of implantation of electrospun PCL scaffolds seeded with rat MSCs (MSC). Sections were stained with H&E (A, C, D, and E) and Safranin O/Fast Green (B). Scale bars in A and B each represent 250 μm, and scale bar in C represents 50 μm in C, D, and E. A and B show mostly fibrous tissue with limited fibrocartilage in the chondral region and new bone growth into the nondegraded PCL scaffold. Round, unstained regions of approximately 10 μm show fibers comprising the PCL scaffold. C, D, and E show high magnification images of the chondral and subchondral regions.

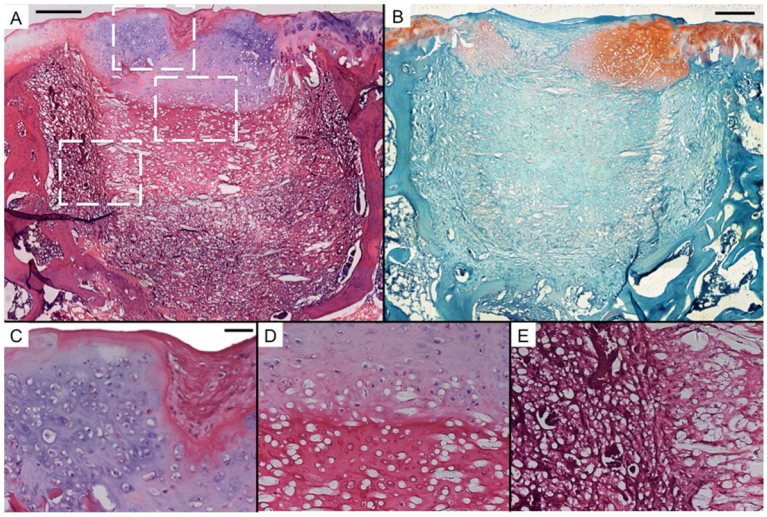

Figure 5.

Representative histological sections of tissue formation after 12 weeks of electrospun PCL scaffolds seeded with a co-culture of rat MSCs and bovine articular chondrocytes (CC). Sections were stained with H&E (A, C, D, and E) and Safranin O/Fast Green (B). Scale bars in A and B each represent 250 μm, and scale bar in C represents 50 μm in C, D, and E. A and B show thick regions of hyaline-like cartilage with some fibrocartilage and fibrous tissue in the chondral region. The subchondral region is composed mainly of transitional and fibrous tissue. Round, unstained regions of approximately 10 μm show fibers comprising the PCL scaffold. C, D, and E show high magnification images of the chondral and subchondral regions.

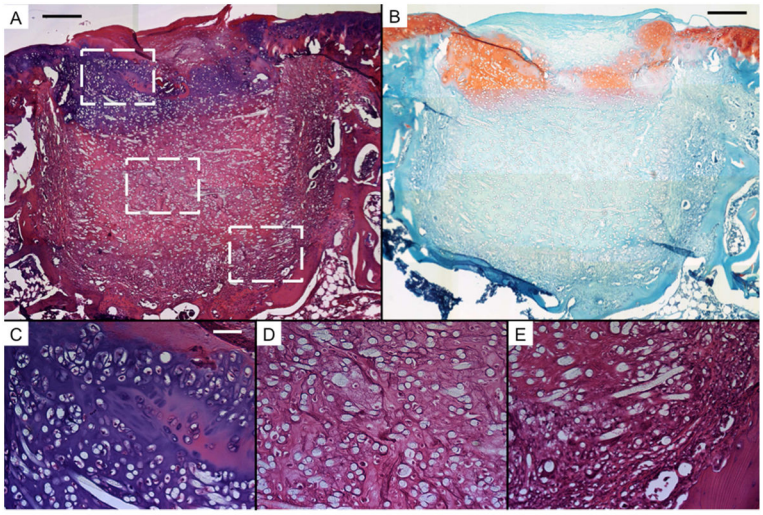

Figure 6.

Representative histological sections of tissue formation after 12 weeks of electrospun PCL scaffolds seeded with bovine articular chondrocytes (AC). Sections were stained with H&E (A, C, D, and E) and Safranin O/Fast Green (B). Scale bars in A and B each represent 250 μm, and scale bar in C represents 50 μm in C, D, and E. A and B show thick regions of hyaline-like cartilage with some fibrocartilage and fibrous tissue in the chondral region. The subchondral region is composed mainly of transitional and fibrous tissue. Round, unstained regions of approximately 10 μm show fibers comprising the PCL scaffold. C, D, and E show high magnification images of the chondral and subchondral regions.

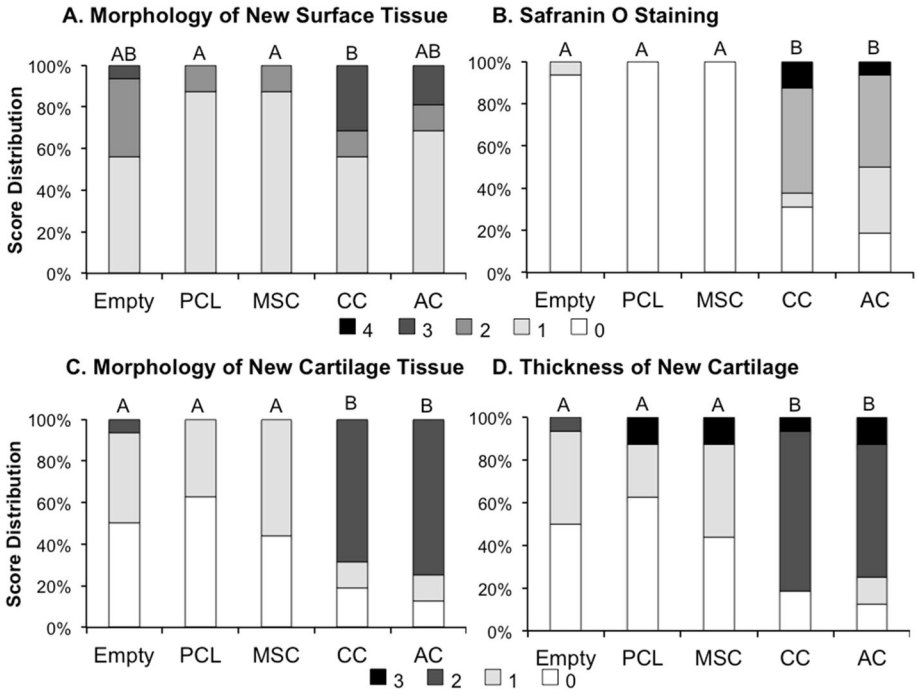

Figure 7.

Histological score distribution for the (A) morphology of new surface tissue, (B) Safranin O staining, (C) morphology of new cartilage, and (D) thickness of new cartilage. Specific scoring criteria for each category is listed in Table 2. Groups not connected by the same letter shown on top of the bars are significantly different ($p<0.05$).

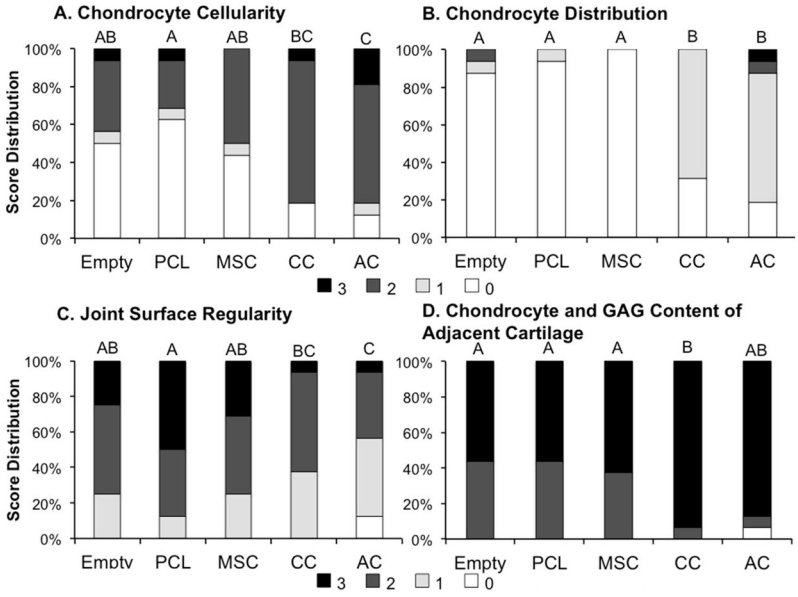

Figure 8.

Histological score distribution for the (A) chondrocyte cellularity, (B) chondrocyte distribution, (C) joint surface regularity, and (D) chondrocyte and GAG content of adjacent cartilage. Specific scoring criteria for each category is listed in Table 2. Groups not connected by the same letter shown on top of the bars are significantly different ($p<0.05$).

Table 1

Outline of experimental groups

Group	Abbreviation	Scaffold	Rat MSCs (cells)	Bovine ACs (cells)
Empty control	Empty	No scaffold	0	0
Material control	PCL	Electrospun PCL	0	0
MSCs	MSC	Electrospun PCL	40,000	0
Co-cultures	CC	Electrospun PCL	30,000	10,000
Articular chondrocytes	AC	Electrospun PCL	0	40,000

Table 2

Histological scoring system for the evaluation of cartilage repair in rat osteochondral defects based off of a modified version of a previously established scoring system for rabbit osteochondral tissue repair (22)

Morphology of New Surface Tissue	
Exclusively AC	4
Mainly hyaline cartilage	3
Fibrocartilage (spherical morphology in >75% of cells)	2
Mostly fibrous tissue (spherical morphology in <75% cells)	1
No tissue	0
Morphology of New Cartilage Tissue	
Exclusively AC	3
Mainly hyaline cartilage	2
Fibrocartilage	1
Only fibrous tissue/ No tissue	0
Thickness of New Cartilage	
Similar to surrounding cartilage	3
Greater than surrounding cartilage	2
Less than surrounding cartilage	1
No cartilage	0
Joint Surface Regularity	
Smooth, intact surface	3
Surface fissures (<25% new surface thickness)	2
Deep fissures (25–99% new surface thickness)	1
Complete disruption of the new surface	0
Chondrocyte Distribution	
Columnar	3
Mixed columnar-clusters	2
Clusters	1
Individual or disorganized cells	0
Chondrocyte Cellularity	
Similar number of chondrocytes	3
More chondrocytes	2
Fewer chondrocytes	1
No chondrocytes	0
Safranin O Staining	
Similar staining intensity	4
Stronger staining intensity	3
Moderate staining intensity	2
Poor staining intensity	1
Little or no staining intensity	0

Chondrocyte and GAG Content of Adjacent Cartilage	
Normal cellularity with normal GAG content	3
Normal cellularity with moderate GAG content	2
Clearly less cells with poor GAG content	1
Few cells with little or no GAGs or no cartilage	0